

# DYNAMICS OF TORQUE CONVERTER WITH LOCK-UP CLUTCH

Takeshi YAMAGUCHI<sup>(a)</sup>, Kazuhiro TANAKA<sup>(b)</sup>, Katsuya SUZUKI<sup>(c)</sup>

<sup>(a)</sup>Aisin AW Co., Ltd. Engineering Division, 10 Takane Fujii-cho Anjyo Aichi, 444-1192, Japan.

<sup>(b)</sup><sup>(c)</sup>Dept. of Mechanical Information Science and Technology, Kyushu Institute Technology, 680-4 Kawazu Iizuka, Fukuoka, 820-8502, Japan

<sup>(a)</sup> [I23962\\_Yamaguchi@aisin-aw.co.jp](mailto:I23962_Yamaguchi@aisin-aw.co.jp), <sup>(b)</sup> [kazuhiro@mse.kyutech.ac.jp](mailto:kazuhiro@mse.kyutech.ac.jp), <sup>(c)</sup> [kachandesu2002@yahoo.co.jp](mailto:kachandesu2002@yahoo.co.jp)

## ABSTRACT

The performance of a torque converter (T/C) has been one of important improvement for an automatic transmission equipped automobile. Improving its performance and efficiency is a key factor to saving fuel consumption. Moreover, the locking up operation or slipping control of an automatic transmission, which makes T/C efficiency higher, is another good opportunity for improving fuel economy. One-dimensional modeling of systems remains effective to recognize a mechanism of the system dynamics. Some bondgraphs models of T/C have been proposed and it becomes more effective for drivability and efficiency to make and add a model for dynamics of the lock-up clutch (L/C). A bondgraphs model of the L/C and a method of calculating parameters through CFD numerical analysis in the components inside T/C are proposed in the present study.

Keywords: torque converter, lock-up clutch, CFD, bondgraphs

## 1. INTRODUCTION

Figure 1 illustrates cut-away view of an automatic transmission, which consists of three major components; the torque converter (T/C), the gearing system and the hydraulic circuit called valve body. The T/C transfers power from the engine to the transmission gearing system and has been used in automatic transmissions for numerous applications such as passenger cars, trucks, buses and trains.

There are two important roles for the T/C. One is the reduction of vibration or noise from the engine by means of the automatic transmission fluid. Another important role is the multiplication of engine torque. Many studies have been carried out to predict hydrodynamic performance and to understand the flow field inside a T/C either experimentally or analytically using Computational Fluid Dynamics (CFD) ((Kim, Ha, Lim, and Cha 2008; Watanabe 1999; Yamaguchi 2002; Abe, Kondoh, Fukumura, and Kojima 1991; Brun and Flack 1995; By and Lakshminarayana 1995; Cigarini and Jonnavithula 1995). The analytical research to date regarding the flow field around the lock-up clutch (L/C) uses CFD simulations performed with steady-state

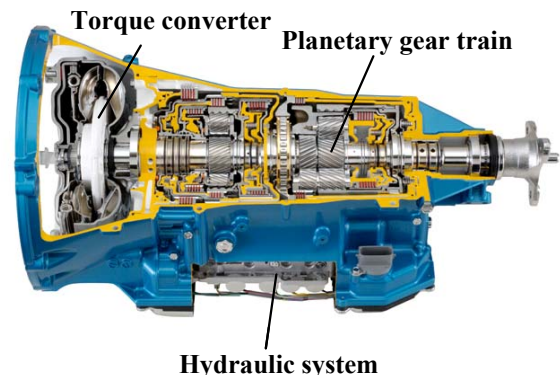


Figure 1: Automatic Transmission (T/C)

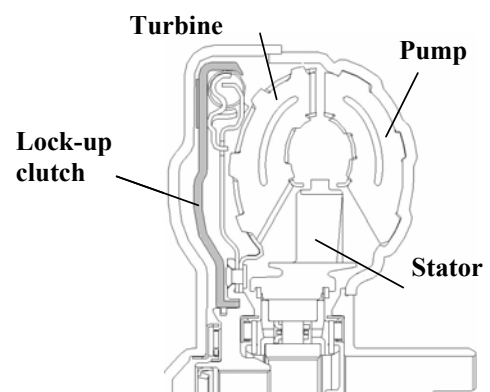


Figure 2: Torque Converter with the Lock-up Clutch

conditions (Ejiri 2006; Abe, Maruyama, Hasegawa and Kondo 1999). A typical automotive T/C cross-section is shown in Fig. 2.

In order to improve the efficiency of an automatic transmission, it is often desired to engage the L/C as soon as possible to conserve the power flow from the engine. However, earlier engagement of the L/C is associated with a larger slip velocity against the input plate, making it increasingly important to manage the heat transfer on the friction paper. Moreover, sudden engagement of the L/C causes vibration and noise within the engine. For this reason, most research has focused either on heat management of the L/C or on the shudder mechanism. The T/C lock-up system is controlled by hydraulics. Understanding from a fluid dynamics perspective how the flow field around the L/C

influences its behavior is a key factor in preventing shock and improving engagement time.

On the other hand, Ishihara introduced theoretical analysis of steady and unsteady characteristics of a T/C (Ishihara and Emori 1966; Hoshino and Ishihara 1990), providing the basic theory of the T/C and the design basis for its development. With the aim of increasing T/C transmission efficiency to meet the demand for higher fuel efficiency vehicles, recently many automobiles have a L/C inside the T/C, which is wet-typed clutch. By using this clutch, input torque is transmitted to both the clutch and fluid divided. If the clutch is working fully, all input torque is transferred through the clutch, and the fluid loss does not occur. Then the T/C efficiency is raised higher. Some researchers have studied the effect of L/C (Tsangarides and Tobler 1985) and slip control (Kono, Itoh, Nakamura, Yoshizawa and Osawa 1995; Hiramatsu, Akagi and Yoneda 1985) of T/Cs. These studies require determination of the dynamic characteristics of T/Cs.

The studies by Ishihara and Emori (1966) have provided the fundamental design method for T/Cs. In developing a practical T/C, however, design engineers apply the design method proposed by Ishihara, which is a complex and time-consuming task. Design engineers, who are expected to achieve higher fuel efficiency design, have been seeking an easier method of analyzing T/C dynamic characteristics. For this demand, a bondgraphs is considered as a better method.

Hrovat and Tobler (1985) applied the bondgraphs method to represent a T/C composed of fluid machinery elements (pump, turbine and stator) without the L/C, based on Ishihara's theory (Ishihara and Emori 1966) on the unsteady characteristics and the bondgraphs model was renewed by Suzuki and Tanaka (2003) with static characteristics of the L/C. By reference to these studies, a bondgraphs model representing the dynamics of the L/C is added to the above-mentioned models and the renewed model becomes a bondgraphs model of the T/C including the dynamic characteristics of the L/C. And CFD numerical analysis has been performed to study the flow structure in various conditions and the L/C engagement time.

## 2. MODELING BY BONDGRAPHS FOR TORQUE CONVERTER

Figure 3 is a bondgraphs representation of basic equations based on the reference (Ishihara and Emori 1966). This bondgraphs contains 4-port I-field, connecting hydraulic elements and mechanical elements via modulated gyrators (MGY). The multi-port I-field is decomposed into single-port I-elements following the procedure by Breedveld (1984), as shown in Fig. 4 (Hrovat and Tobler 1985; Suzuki and Tanaka 2003). The bondgraphs, which may look complex, is easy to understand in terms of correspondence to actual components. With the bondgraphs of Fig. 4, it is easy to find the correspondence between the bondgraphs elements for pump, turbine and stator and actual

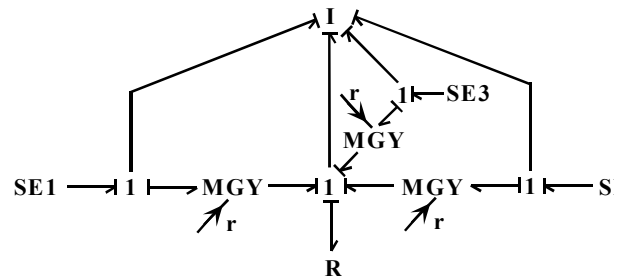


Figure 3: Bondgraphs for T/C

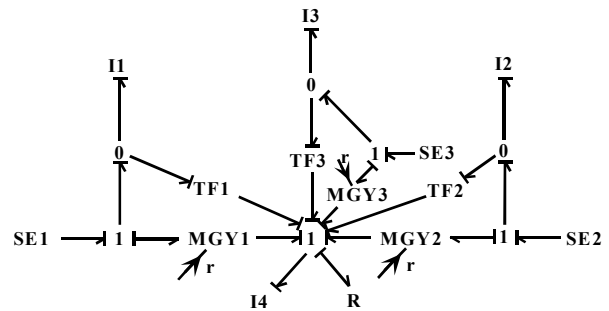


Figure 4: Decomposed Bondgraphs

counterparts. Each symbol is suffixed with an identification number: 1, 2 and 3 represents pump, turbine and stator elements, respectively. All of these elements are connected via the 1-junction in the lower center of the bondgraphs, indicating that the flow rate in the pump, turbine and stator is the same at this 1-junction. Pressure loss caused by shock and friction is represented by R-element, indicating that the pressure loss can be obtained from the flow rate represented by 1-junction for each impeller. From the conservation law of angular momentum, the following three equations of motion can be obtained for the respective impellers,

For pump:

$$T_1 = I_1 \dot{\omega}_1 - \rho S_1 \dot{Q} + \rho Q \{ (r_2 \omega_1 - c_2 \tan \alpha_{12}) r_2 - (r_1 \omega_3 - c_1 \tan \alpha_{32}) r_1 \} \quad (1)$$

For turbine:

$$T_2 = I_2 \dot{\omega}_2 - \rho S_2 \dot{Q} + \rho Q \{ (r_3 \omega_2 - c_3 \tan \alpha_{22}) r_3 - (r_2 \omega_1 - c_2 \tan \alpha_{12}) r_2 \} \quad (2)$$

For stator:

$$T_3 = I_3 \dot{\omega}_3 - \rho S_3 \dot{Q} + \rho Q \{ (r_1 \omega_3 - c_1 \tan \alpha_{32}) r_1 - (r_3 \omega_2 - c_3 \tan \alpha_{22}) r_3 \} \quad (3)$$

Here,  $\rho S_i \dot{Q}$  represents change in momentum of fluid existing in impeller; the dot indicates differential by time;  $S_i$  is a constant determined by the blade configuration (Ishihara and Emori 1966).

According to the conservation law of kinetic energy, the rate of kinetic energy increases  $\dot{E}_k$  of fluid per unit time is represented by the following equation:

$$\dot{E}_k = T_1 \omega_1 + T_2 \omega_2 + T_3 \omega_3 - \dot{E}_l \quad (4)$$

where  $\dot{E}_l$  is energy loss of flow per unit time.

Therefore, another equation of motion holds as follows:

$$\begin{aligned} & \rho\Phi\dot{Q} - \rho(S_1\dot{\omega}_1 + S_2\dot{\omega}_2 + S_3\dot{\omega}_3) \\ & = \rho\{(r_2\omega_1 - c_2 \tan \alpha_{12})r_2 - (r_1\omega_3 - c_1 \tan \alpha_{32})r_1\}\omega_1 \quad (5) \\ & + \rho\{(r_3\omega_2 - c_3 \tan \alpha_{22})r_3 - (r_2\omega_1 - c_2 \tan \alpha_{12})r_2\}\omega_2 \\ & + \rho\{(r_1\omega_3 - c_1 \tan \alpha_{32})r_1 - (r_3\omega_2 - c_3 \tan \alpha_{22})r_3\}\omega_3 - P_L \end{aligned}$$

where  $\Phi$  is a constant and can be defined as follows according to the blade configuration:

$$\Phi = \oint \sec^2 \alpha dl \quad (6)$$

$P_L$  is a pressure loss defined by  $\dot{E}_l = QP_L$ , and is equal to the sum of shock loss and frictional loss, as expressed by Eq. (7). The coefficient of the shock loss is assumed to be 1.0 (Ishihara and Emori 1966).

$$\begin{aligned} P_L = & 1/2 \rho [ \{(r_1\omega_1 - c_1 \tan \alpha_{11}) - (r_1\omega_3 - c_1 \tan \alpha_{32})\}^2 \\ & + \{(r_2\omega_2 - c_2 \tan \alpha_{21}) - (r_2\omega_1 - c_2 \tan \alpha_{12})\}^2 \\ & + \{(r_3\omega_3 - c_3 \tan \alpha_{31}) - (r_3\omega_2 - c_3 \tan \alpha_{22})\}^2 + Lc_2^2 ] \quad (7) \end{aligned}$$

Here,

$$L = \sum_{i=1}^3 \lambda_i \{1 + (\tan^2 \alpha_{i1} + \tan^2 \alpha_{i2})/2\} \quad (8)$$

where  $\lambda_i$  is a loss coefficient.

In the above equations, the torque and angular velocity in a mechanical system component, and the pressure and flow rate in a hydraulic system, correspond to the effort and flow variables, respectively, of the bondgraphs. This correspondence can be expressed explicitly using a matrix notation as follows:

$$\mathbf{I}\dot{\mathbf{f}} = -\mathbf{G}(\mathbf{f})\mathbf{f} - \mathbf{R}(\mathbf{f}) + \mathbf{T} \quad (11)$$

where  $\mathbf{f}$  is the matrix of the flow variables in the system bondgraphs, as expressed below:

$$\mathbf{f} = [\omega_1 \quad \omega_2 \quad \omega_3 \quad Q]^T \quad (12)$$

$\mathbf{I}$  is the matrix of inertial moment, as expressed below:

$$\mathbf{I} = \begin{bmatrix} I_1 & 0 & 0 & -\rho S_1 \\ 0 & I_2 & 0 & -\rho S_2 \\ 0 & 0 & I_3 & -\rho S_3 \\ -\rho S_1 & -\rho S_2 & -\rho S_3 & \rho\Phi \end{bmatrix} \quad (13)$$

$\mathbf{G} = \mathbf{G}(\mathbf{f})$  is the matrix of a modulated gyrator, as expressed below:

$$\mathbf{G} = \mathbf{G}(\mathbf{f}) = \begin{bmatrix} 0 & g^T \\ -g & 0 \end{bmatrix} \quad (14)$$

$$\mathbf{g} = \mathbf{g}(\mathbf{f}) = [\rho g_1 \quad \rho g_2 \quad \rho g_3] \quad (15)$$

where

$$g_1 = \{(r_2\omega_1 - c_2 \tan \alpha_{12})r_2 - (r_1\omega_3 - c_1 \tan \alpha_{32})r_1\} \quad (16)$$

$$g_2 = \{(r_3\omega_2 - c_3 \tan \alpha_{22})r_3 - (r_2\omega_1 - c_2 \tan \alpha_{12})r_2\} \quad (17)$$

$$g_3 = \{(r_1\omega_3 - c_1 \tan \alpha_{32})r_1 - (r_3\omega_2 - c_3 \tan \alpha_{22})r_3\} \quad (18)$$

$\mathbf{R} = \mathbf{R}(\mathbf{f})$  is the matrix of loss, as follows:

$$\mathbf{R} = \mathbf{R}(\mathbf{f}) = [0 \quad 0 \quad 0 \quad P_L]^T \quad (19)$$

$\mathbf{T}$  is the matrix of torque applied by each impeller to fluid, as expressed below:

$$\mathbf{T} = [T_1 \quad T_2 \quad T_3 \quad 0]^T \quad (20)$$

From the assumption that cross sectional area of flow passage is constant,  $c_1 = c_2 = c_3 = Q/A$  in all of the above equations.

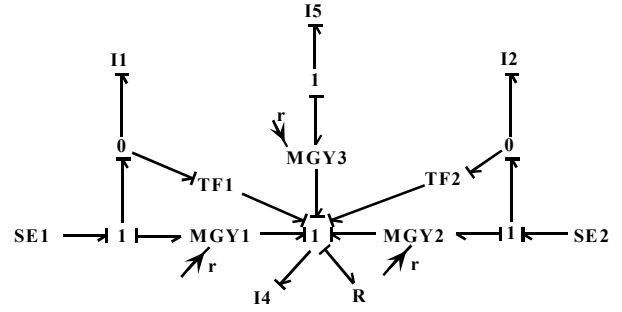


Figure 5: Bondgraphs for Converter Range

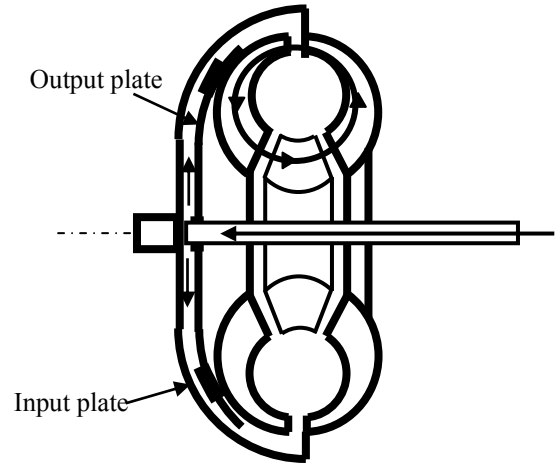


Figure 6: Torque Converter with a Lock-up Clutch

In the converter range, a stator is fixed and not rotating. However, since a stator is generally shaped as a blade, it produces a torque as the result of change in momentum, which is determined by the inlet and outlet blade angles. This torque is received by the transmission case. Fluid is then forced by the reaction torque to return along the blade surface to the pump inlet side. When these characteristics are represented by a bondgraphs, TF-element for a stator and the bond connecting to this element are omitted, and I3-element is combined with I-element for a transmission case to become I5-element, as shown in Fig. 5. Normally, when a transmission torque is transmitted, the corresponding torque reaction works on the casing, as shown in Fig. 5 (Suzuki and Tanaka 2003). As mentioned above, since torques work on the stator, stator-related bonds should be included in the bondgraphs to represent a T/C accurately.

### 3. LOCK-UP CLUTCH IN T/C

Many automobiles have the lock-up clutch (L/C) in a T/C shown in Fig. 6. The L/C is a wet-type friction clutch and consists of an input plate and an output plate. The input clutch is connected to the pump impeller and the output clutch is connected to the turbine runner. If the clutch is engaged, its revolution is the same as the pump and the turbine. Then a bond of the input plate is connected to 1-junction of the pump. Between input and output plate the oil flows. This flow is controlled by a regulator valve outside the T/C. If the regulator valve is closed, the clutch is working and it transmits the torque.



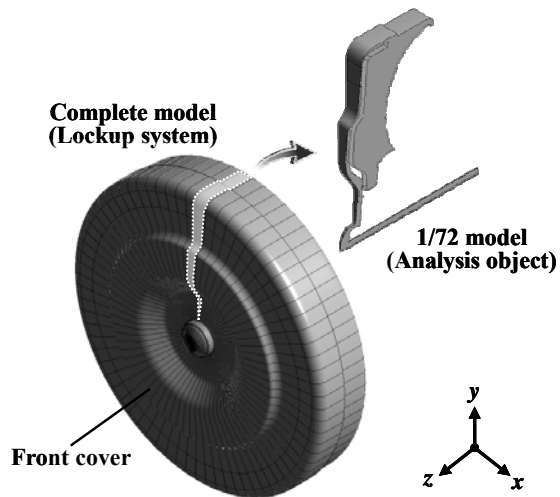


Figure 9: Analysis Object of the Lock-up System

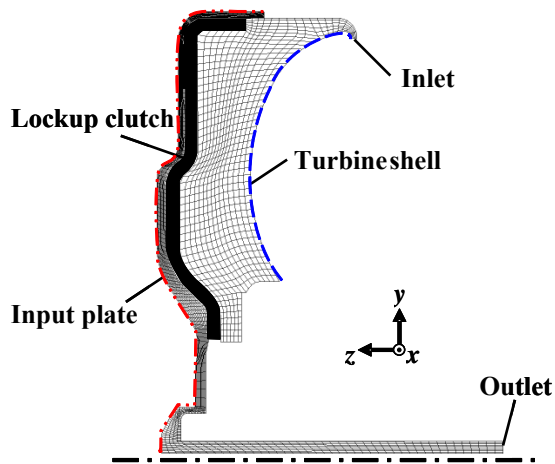


Figure 10: Computational Grids of the Lock-up Clutch

#### 4. MODEL DESCRIPTION AND NUMERICAL ANALYSIS FOR L/C DYNAMICS

For the CFD analysis, the object of the lock-up system is shown in Fig. 9, and the CFD model of the L/C is shown in Fig. 10. Since this problem is axis-symmetric, only seventieth part of the L/C is modeled with periodical boundary conditions to reduce time spent on computation. Here, it is assumed that the flow field around the L/C is independent of the flow field inside the torus (i.e., pump, turbine, and stator blade area). Therefore, the torus was not included in this model. The speed ratio is defined as the turbine rotational speed divided by the pump rotational speed. The pump rotational speed is simulated by rotating the entire calculated domain, and the turbine rotational speed is simulated by rotating the walls of the model as defined by the L/C and the turbine shell.

Figure 11 shows the boundary conditions for inlet and outlet pressure used for this simulation. At the beginning, the outlet pressure is higher than the inlet pressure. The resulting differential pressure prevents the L/C from moving. The inlet pressure then increases quadratically, and the outlet pressure decreases linearly. This variation in pressure is a typical lock-up control

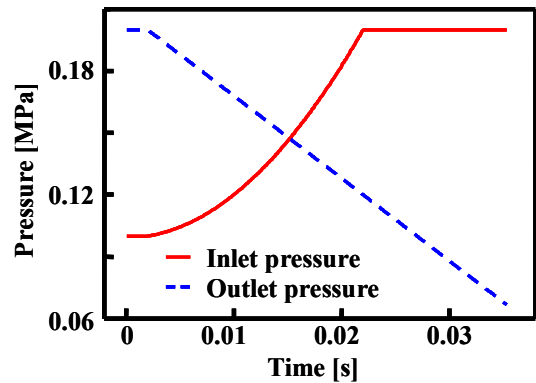


Figure 11: Inlet and Outlet Pressure Distribution

Table 1: Analysis Conditions for Transient State

|                          |                            |
|--------------------------|----------------------------|
| Pump rotational speed    | 2000 rpm                   |
| Turbine rotational speed | 1600, 1800, 2200, 2400 rpm |
| Speed ratio              | 0.8, 0.9, 1.1, 1.2         |
| Inlet pressure           | Solid line of Fig. 11      |
| Outlet pressure          | Dashed line of Fig. 11     |

sequence used for actual automatic transmissions. The boundary conditions for this simulation are summarized in Table 1. Because the lock-up system begins to engage when the speed ratio, which indicates the ratio of turbine rotational speed to pump rotational speed and is represented by  $e$ , becomes more than 0.7 or 0.8, the simulations were performed in case of  $e \geq 0.8$ .

ANSYS CFX Ver12.1 is used for the CFD solver. In this simulation, the lock-up motion is not known a priori and will be calculated based on the forces acting on the L/C according to Newton's Second Law. The motion equation is re-assembled and translated to CFX CEL (CFX Expression Language). The Navier–Stokes equations can then be solved and specified explicitly with this CEL. In reality, the friction paper on the L/C contacts the input plate to transfer torque. However, in the simulation, contact of the friction paper would violate the continuity equation and would either collapse or diminish the CFD mesh. In order to maintain fluid continuity and prevent the mesh from collapsing, a small gap is set between the L/C and the input plate. Since the friction paper is on the L/C, a minimum clearance of 0.1 mm is set between the friction paper and the input plate. The initial clearance is bounded at 1.3 mm, meaning the L/C travels from 1.3 mm to the 0.1 mm minimum gap.

Another new technique was introduced to keep the mesh quality constant. Instead of using a CAD rendering of the initial shape of the L/C to mesh the model, a CAD rendering of the final deflected shape at the minimum clearance of 0.1 mm ( $s = 0.1$  mm) was meshed and then extended 1.3 mm ( $s = 1.3$  mm) in the direction of movement to its initial position. This technique maintained good quality of the moving mesh and prevented divergence during the simulation. The number of numerical mesh is 11,000 elements, all of the hexahedral type.

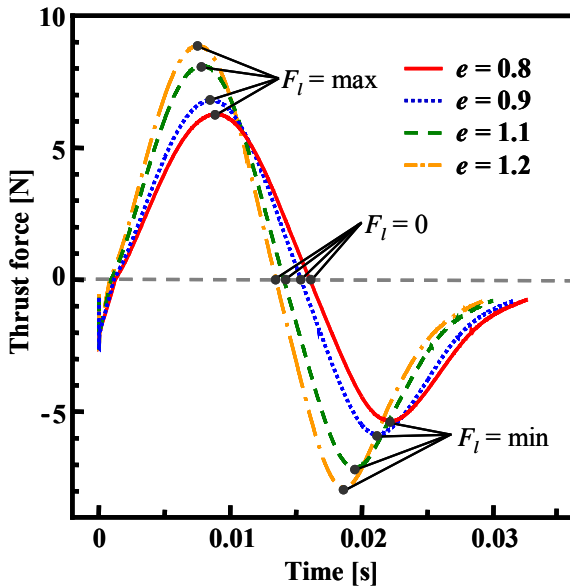


Figure 12: Thrust Force of the Lock-up Clutch

## 5. RESULTS AND DISCUSSIONS

Figure 12 shows the thrust force acting on the L/C over time at various speed ratios. In this simulation, the pump rotational speed is fixed at 2000 rpm, and the turbine speed is varied to achieve the different speed ratios. Thus, the turbine speed is 1600 rpm for  $e = 0.8$  and 2400 rpm for  $e = 1.2$ . Negative thrust force values act to separate the L/C from the input plate. Before the inlet pressure exceeds the outlet pressure, the thrust force acting on the clutch is negative, and the clutch holds steady. After engagement pressure is applied, the thrust force becomes positive and increases until it reaches a maximum inflection point. After passing this point, the thrust force gradually decreases to a minimum inflection point and then increases again. This trend is true at all speed ratios. The maximum inflection point, the minimum inflection point, and the point where the thrust force becomes zero are defined as  $F_l = \max$ ,  $F_l = \min$  and  $F_l = 0$ , respectively.

Comparing the data in Fig. 12 at speed ratio  $e = 0.8$  and 1.2, the maximum and minimum thrust forces have greater absolute values at the higher speed ratio than at the lower speed ratio. The shear stress induced in the working fluid by both the input plate wall and the L/C wall imparts momentum energy to the working fluid. Since the rotational speed of the input plate (pump rotational speed) is fixed, the difference in the momentum of the working fluid is due to the L/C speed (turbine speed).

Figure 13 shows the L/C movement from the initial condition (lock-up off position) with various speed ratios. The pump rotational speed is fixed at 2000 rpm. The L/C is in its initial position at  $s = 1.3$  mm and is at its final engagement point at  $s = 0.1$  mm. At each speed ratio, even though the inlet pressure continues to increase, the L/C does not begin to move until 0.005 sec. Once movement begins, the displacement grows quadratically until the L/C reaches its final engagement point. In addition, when the thrust force reaches

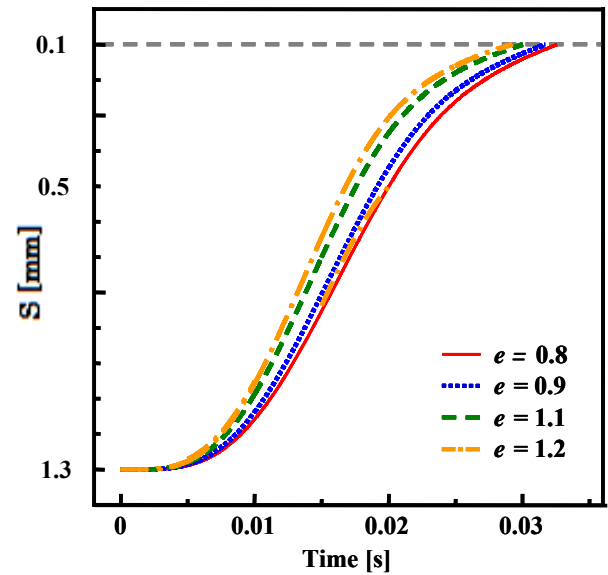


Figure 13: Lock-up Clutch Moving Distance

minimum inflation point in Fig. 12, the inflation point also can be seen at the same time in Fig.13. Moreover, the higher speed ratios, the engagement time is reduced. At lower speed ratios, the slipping speed is higher, and more shear flow or more energy is created in the working fluid. Higher pressure is required to overcome the additional energy in the working fluid at lower speed ratios. However, since the inlet pressure is limited by the boundary conditions of the simulation (see Fig. 11), the engagement time required to overcome the additional energy at lower speed ratios is increased.

Figure 14 shows the pressure distribution in the meridian plane of the L/C for  $e=0.8$  at three different values of thrust force: (a)  $F_l = \max$ , (b)  $F_l = 0$ , and (c)  $F_l = \min$ . In Fig. 14 (a), the outlet pressure is still higher than the inlet pressure due to the initial condition of the simulation. At the same time, the pressure increases in the radial direction due to centrifugal pressure. The pressure at the turbine shell is higher than the pressure at the input plate. This pressure difference, shown in Fig. 14 (a), creates a positive thrust force and acts to engage the L/C as previously discussed. Figure 14 (b) shows that the pressure distribution at the input plate and at the turbine shell is equivalent. Since there is no thrust force acting on the L/C, only inertia is driving the movement of the L/C. In Fig. 14 (c), the pressure distribution at the input plate becomes higher than at the turbine shell. The velocity of the L/C is reduced by the higher pressure at the input plate. The maximum and minimum pressure differences across the L/C coincide with the inflection points in Fig. 12.

Figure 15 shows the limiting streamlines on the input plate and the friction paper at speed ratio 0.8 and 1.2 with  $F_l = \min$  condition. Over all, due to the inlet pressure driven radial flow and centrifugal force, the flow tends to move left-bottom side to right-top side. At  $e=0.8$ , the rotational velocity of the input plate is higher than that of the friction paper (the L/C). As a result, the limiting streamlines on the input plate tend to move

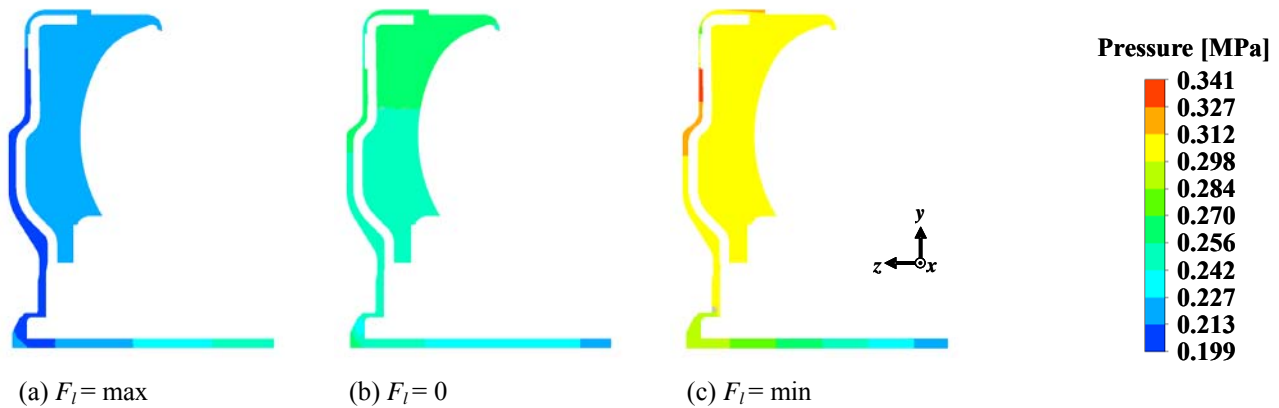


Figure 14: Pressure Distributions in the Meridian Plane ( $e = 0.8$ )

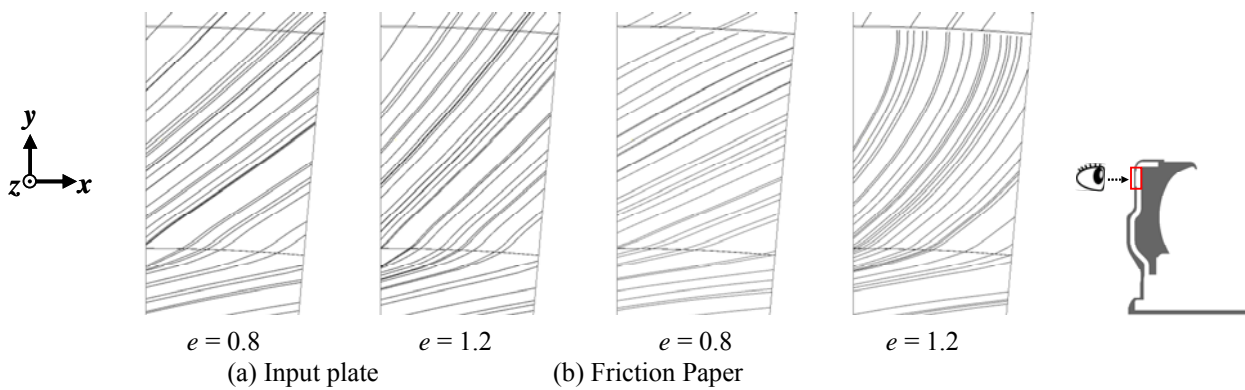


Figure 15: Streamline on the Input plate and the Friction Paper at  $F_l = \min$

more upward compared to the friction paper side. For the same reason, at  $e = 1.2$ , the limiting streamlines on the friction paper move more upward.

As mentioned above, the flow field around the L/C can be perfectly simulated. At this stage, it finally becomes possible to determine appropriately the value of every R-element shown in Fig. 8 which has relations with pressure loss in the flow passage around the L/C.

## 6. CONCLUSIONS

A proposed bondgraphs has been applied to represent the functions of a torque converter. This bondgraphs can accurately represent dynamics of the lock-up clutch and enables easy correspondence between the bondgraphs model for the torque converter and explanation of the physical phenomena occurring in the torque converter. By use of this bondgraphs it becomes possible to control the lock-up clutch in dynamic characteristics, especially in slip control of the torque converter.

The flow field around the lock-up clutch has been simulated with a commercial CFD code. It has been found that the motion of the lock-up clutch is not linear, and that a small gap between the output plate and the input plate has an enormous effect on the lock-up clutch engagement time and on the flow field. The effects of the speed ratio, the pressure distribution, the streamlines in the meridian plane and the streamlines on the input plate and the friction paper have been studied.

The flow structures in the meridian plane are generally the same at the time that the thrust force becomes maximum or minimum, even at different speed ratio.

As a result that the flow field around the lock-up clutch is simulated numerically, it finally becomes possible to determine appropriately the value of every R-element which has relations with pressure loss in the flow passage around the lock-up clutch. At this stage, the proposed new bondgraphs model enhances its reality.

## REFERENCES

- Abe, K., Kondoh, T., Fukumura, K., and Kojima, M., 1991. Three-Dimensional Simulation of the flow in a Torque Converter. *SAE Paper No. 910800*.
- Abe, H., Maruyama, T., Hasegawa, K., and Kondo, N., 1999. Analyzing Responsiveness of lock-up Clutch by Applying Three Dimensional Computational Fluid Dynamics. *HONDA R&D Technical Review*, Vol. 11 No2. pp.67-72.
- Breedveld, P.C., 1984. Decomposition of Multiport Elements in a Revised Multibondgraph Notation. *J. Franklin Inst.*, Vol. 318: pp.253-273.
- Brun, K., Flack, R. D., 1995. Laser Velocimeter Measurements in the Turbine of an Automotive Torque Converter: Part II-Unsteady Measurements. *ASME paper 95-GT-293*.

- By, R. R., Lakshminarayana, B., 1995. Measurement and Analysis of Static Pressure Field in a Torque Converter Pump. *Trans. of ASME, J. Fluids Eng.*, Vol. 117: pp.109-115.
- Cigarini, M., Jonnavithula, S., 1995. Fluid Flow in an Automotive Torque Converter: Comparison of Numerical Results with Measurements. *SAE Technical Paper* No. 950673.
- Ejiri, E., 2006. Analysis of Flow in a Lock-up Clutch of an Automotive Torque Converter. *JSME International Journal*, Series B 49(1). pp.131-141.
- Hiramatsu, T., Akagi, T., and Yoneda, H., 1985. Control Technology of Minimal Slip-type Torque Converter Clutch. *SAE Tech. Paper* No. 850460.
- Hoshino, A., Ishihara, T., 1990. A Consideration on Performance Improvement of Hydraulic Torque Converters. *Trans. of ASME*, Vol. 100: pp.65-70.
- Hrovat, D., Tobler, W. E., 1985. Bondgraph Modeling and Computer Simulation of Automotive Torque Converters. *J. of Franklin Inst.*, Vol. 319-1/2: pp.93-114.
- Ishihara, T., Emori, R. I., 1966. Torque Converter as a Vibrator Damper and Its Transient Characteristics. *SAE Paper* No. 660368.
- Kim B S., Ha, S. B., Lim, W. S., and Cha, S. W., 2008. Performance Estimation Model of a Torque Converter Part 1: Correlation between the Internal Flow Field and Energy Loss Coefficient. *International Journal of Automotive Technology* Vol. 9, No. 2: pp.141-148.
- Kono, K., Itoh, H., Nakamura, S., Yoshizawa, K., and Osawa, M., 1995. Torque Converter Clutch Slip Control System. *SAE Tech. Paper* No. 950672.
- Suzuki, K., Tanaka, K., 2003. Torque Converter with Lock-up Clutch by Bond Graphs. *Proceedings of ICBGM2003*. January 19-23, Orlando, Florida.
- Tsangarides, M. C., Tobler, W. E., 1985. Dynamic Behavior of a Torque Converter with Centrifugal Bypass Clutch. *SAE Paper* No. 850461.
- Watanabe, H., 1999. Flow Visualization and Measurement in the Stator of Torque Converter. *Toyota Central Labs R&D Review* Vol. 34, No. 1. pp.57-66.
- Yamaguchi, T., 2002. Automotive Torque Converter Performance Prediction Using a New CFD Approach. *Proceedings of The 9<sup>th</sup> of International Symposium on Transport Phenomena and Dynamics of Rotating Machinery (ISROMAC-9)*, February 10-14, Honolulu, Hawaii.

#### **AUTHORS BIOGRAPHY**

##### **TAKESHI YAMAGUCHI,**

He graduated from Tohoku University, and obtained M.S. in San Diego State University. After working at Tohoku University as an assistant professor, he became a chief engineer in Aisin AW and also a Ph.D. candidate now. He has wide interests in CFD analyses and development on an automatic transmission as well as the basic phenomena of fluid mechanics. He is also a good scuba diver.

##### **KAZUHIRO TANAKA,**

He graduated from the University of Tokyo, obtained the first job as an assistant professor in Sophia University, and moved back to the University of Tokyo. After then, he moved to Kyushu Institute of Technology and is a professor. He has interests in combining Bondgraphs modeling and simulation with CFD analyses on flow patterns inside various components and systems.

##### **KATSUYA SUZUKI**

He retired from Toyota Motor Corporation, where he was a project general manager of Drive Train Division. He obtained Ph.D. degree in Nagoya University. He is now a visiting professor in Kyushu Institute of Technology and enjoys a lively discussion of Bondgraphs modeling and simulation. He is a member of a chorus group singing the Ninth Symphony in Nagoya.